Progress in Organic Coatings 47 (2003) 384–392

PROGRESS IN ORGANIC COATINGS

www.elsevier.com/locate/porgcoat

Nanoparticle-filled silane films as chromate replacements for aluminum alloys

Vignesh Palanivel, Danqing Zhu, Wim J. van Ooij*

Department of Materials Science and Engineering, University of Cincinnati, Cincinnati, OH 45221-0012, USA

Abstract

Silane surface treatments have been developed as an alternative for toxic and carcinogenic chromate-based treatments for years. It is consistently observed that ultra-thin silane films offer excellent corrosion protection as well as paint adhesion to metals. The silane performance is comparable to, or in some cases better than, that of chromate layers. The most recent studies also showed that the silane films can be thickened and strengthened by loading of a small amount of nanoparticles such as silica and alumina into the films resulting in enhanced corrosion protection of aluminum alloys.

Keywords: Ultra-thin silane film; Aluminum alloy; Nanoparticles

1. Introduction

Recently, silane surface treatment has evolved as a promising alternative for toxic chromate-based treatments in metal-finishing industries [1–8]. The studies concerning corrosion protection of metals using silane films have invariably demonstrated that silanes, a group of environmentally compliant chemicals, could efficiently protect metals against different forms of corrosion in two major ways. That is, (1) a single silane film can protect metals against corrosion without topcoats for 6 months to 1 year, and (2) silanes can also be used in surface pretreatments of metals before painting. In the former case, the thickness of silane films is normally around 200–400 nm obtained from 5% silane solutions. In the latter case, the as-deposited ultra-thin silane layers (∼100 nm) from 2% silane solutions perform excellently as a paint adhesion promoter as well as a corrosion retardant under different topcoats such as epoxies, polyurethanes, polyesters and acrylics.

Trialkoxysilanes (or silanes) with the general formula of $R'(CH_2)_nSi(OR)_3$ (where R′ denotes organic functionality, and OR indicates hydrolyzable alkoxy group, e.g. methoxy (OCH_3) or ethoxy (OC_2H_5)), have been widely used as adhesion promoters in paints, fillers, and binders in the industry of glass/polymer composites for a long time. The studies of silanes as adhesion promoters have been conducted extensively by the adhesion scientific community in the past few decades. An abundance of silane theories have been well-documented [9–11]. According to these studies, a general accepted bonding mechanism of silanes to metal surfaces is illustrated in Fig. 1 [12]. When dipping a metal into a dilute silane solution (e.g. 2–5 vol.%) for a few seconds, silanols (SiOH) in the silane solution adsorb spontaneously onto the metal surface through hydrogen bonds, as shown in Fig. 1(a). Upon drying, there are two key condensation reactions occurring at the silane/metal interfacial region. SiOH groups from the silane solution and the metal hydroxyls (MeOH) from the metal surface hydroxide form covalent metallo-siloxane bonds (MeOSi) according to

$$SiOH_{(solution)} + MeOH_{(metal\ surface)} = SiOMe_{(interface)} + H_2O \quad (1)$$

The excess SiOH groups adsorbed on the metals would also condense among themselves to form a siloxane (SiOSi) film

$$SiOH_{(solution)} + SiOH_{(solution)} = SiOSi_{(silane\ film)} + H_2O \quad (2)$$

The as-formed MeOSi and SiOSi covalent bonds are assumed to be responsible for the excellent bonding of the silane film to the metal substrate (Fig. 1).

It has also been demonstrated in the previous studies that bis-silanes such as bis-[3-(triethoxysilylpropyl)]ethane (BTSE, $(OC_2H_5)_3Si(CH_2)_2Si(OC_2H_5)_3$) and bis-[3-(triethoxysilyl)propyl]tetrasulfide (bis-sulfur silane, $(OC_2H_5)_3Si(CH_2)_3S_4(CH_2)_3–Si(OC_2H_5)_3$) performed much better in terms of corrosion protection as compared with

* Corresponding author. Tel.: +1-513-556-3194; fax: +1-513-556-3773.
E-mail address: vanooiwj@email.uc.edu (W.J. van Ooij).

0300-9440/$ – see front matter © 2003 Elsevier B.V. All rights reserved.
doi:10.1016/j.porgcoat.2003.08.015

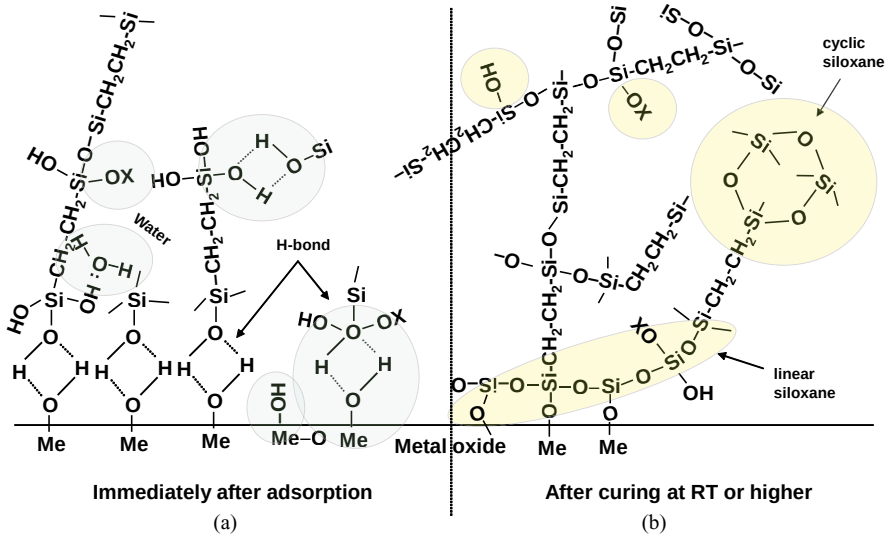

Fig. 1. Simplified schematic of bonding mechanism between silane molecules and metal surface hydroxide layer: (a) before condensation: hydrogen-bonded interface; (b) after condensation: covalent-bonded interface.

mono-silanes [2–5]. The major difference between these two types of silanes is that the number of hydrolyzable OR groups in a bis-silane molecule doubles that in a mono-silane molecule, as illustrated in Fig. 2 [12]. A mono-silane molecule only has three OR groups attached to the silicon (Si) atom at one end (Fig. 2(a)), whereas a bis-silane molecule has six OR groups in total and two Si atoms at both ends, with every three OR groups attached to a Si atom (Fig. 2(b)). It was further noted in our previous studies [2–5] that the bis-silanes tend to bond to metal substrates more tightly than the mono-silanes. The former with more OR groups is able to develop a much denser interfacial region through the above two reactions (1) and (2) than the latter a more detailed explanation regarding this aspect was given elsewhere [12].

BTSE and bis-sulfur silanes exhibit outstanding corrosion protection performance on Al alloys such as AA 2024-T3, AA 6061-T6, AA 5005 and AA 7075-T6 without topcoats. An example is given in Fig. 3, which shows that bis-sulfur silane-treated AA 2024-T3 panel survived 504 h of salt spray test (SST) without showing any significant corrosion activity on the metal surface (Fig. 3(c)). The untreated and chromated (Alodine® 2000 process) panels (Fig. 3(a) and (b)) were used here as the controls. Similar to the silane-treated surface, the chromated surface has also been protected very well. Nevertheless, it should be pointed out that the bis-sulfur silane film obtained from a 5% silane solution is about 400 nm thick. While the chromate obtained in the Alodine process has a typical thickness of greater than 1000 nm. Thus, silane films outperform chromate films on a per-weight basis.

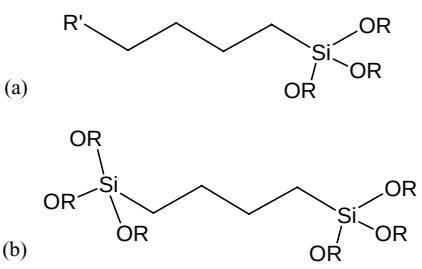

Fig. 2. Structures of bis-silane molecule (a) and mono-silane molecule (b).

In addition to the anticorrosive efficiency, another major concern of the use of silane films is the mechanical properties of such films. In service, these silane films on metals should be capable of resisting mechanical damages by impact, scratch and wear. Therefore, one of our current research subjects is to improve mechanical properties of silane films by loading nanoparticles into the films.

A preliminary study on this aspect was done on AA 5005 treated with a water-based silane (i.e. a mixture of bis-amino silane and vinyltriactoxysilane (VTAS)) loaded with a small amount of alumina nanoparticles obtained from the 5% silane solution containing 50 ppm alumina. The 336 h-SST results are shown in Fig. 4. It is seen that the corrosion protection offered by the nano-structured silane film (Fig. 4(c)) is comparable to that of the chromate layer (Fig. 4(b)). No corrosion has been found on both treated alloy surfaces (Fig. 4(b) and (c)). The untreated surface in Fig. 4(a), on the other hand, has corroded heavily. Most recently, a systematic study has been done by using nanoparticle-loaded bis-sulfur silane films on AA 2024-T3 substrates, where the nanoparticles were colloidal silica. The results are reported here.

2. Experimental

2.1. Materials

Silane. bis-[3-(triethoxysilyl)-propyl]tetrasulfide (or bis-sulfur silane), with the trade name of Silquest A-1289®,

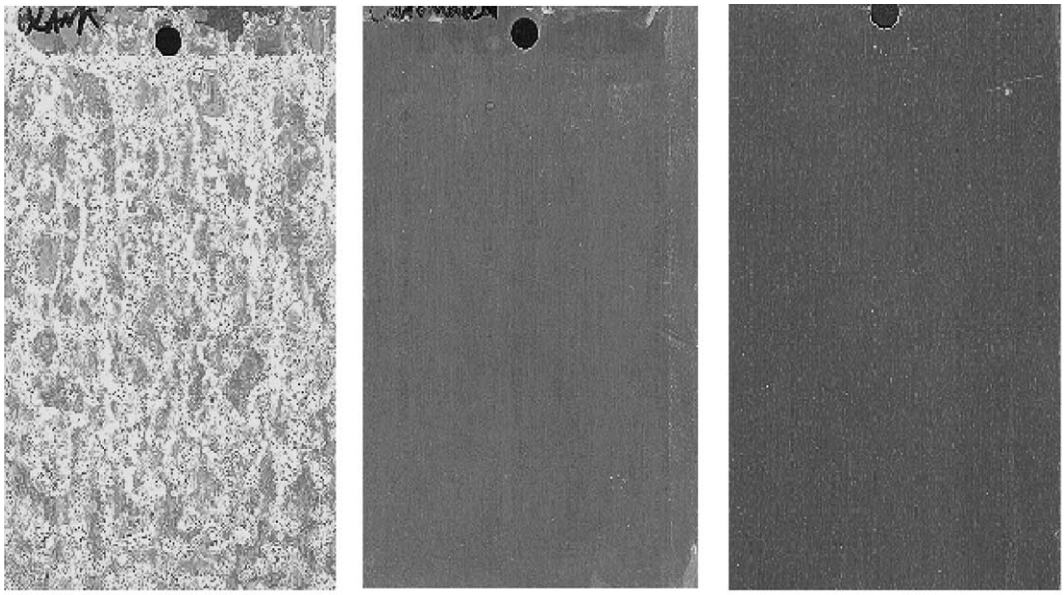

Fig. 3. AA 2024-T3 panels after 504 h of salt spray test: (a) untreated; (b) chromated (CHEM-CODE 105®); (c) bis-sulfur silane treated.

was provided by OSi Specialties (Tarrytown, NY). The silane was used without further purification. Before application, the OR groups of the silane need to be converted to active SiOH groups for the subsequent condensation reactions. The conversion of the OR groups is usually realized by hydrolyzing the silane in its diluted aqueous solution.

In this work, a 5 vol.% bis-sulfur silane solution was prepared by adding the silane to a mixture of deionized (DI) water and ethanol. The ratio of bis-sulfur silane/DI water/ethanol was 5/5/90 (v/v/v). The natural pH of the solution was 6.5. The solution was stirred for 10 min, and then aged in ambient conditions for at least 2 days to ensure that the solution became "functional" [13]. In other words, a sufficient number of active SiOH groups were generated in the solution for the condensation reactions. In this way, a solid rather than an oily silane film can be formed on

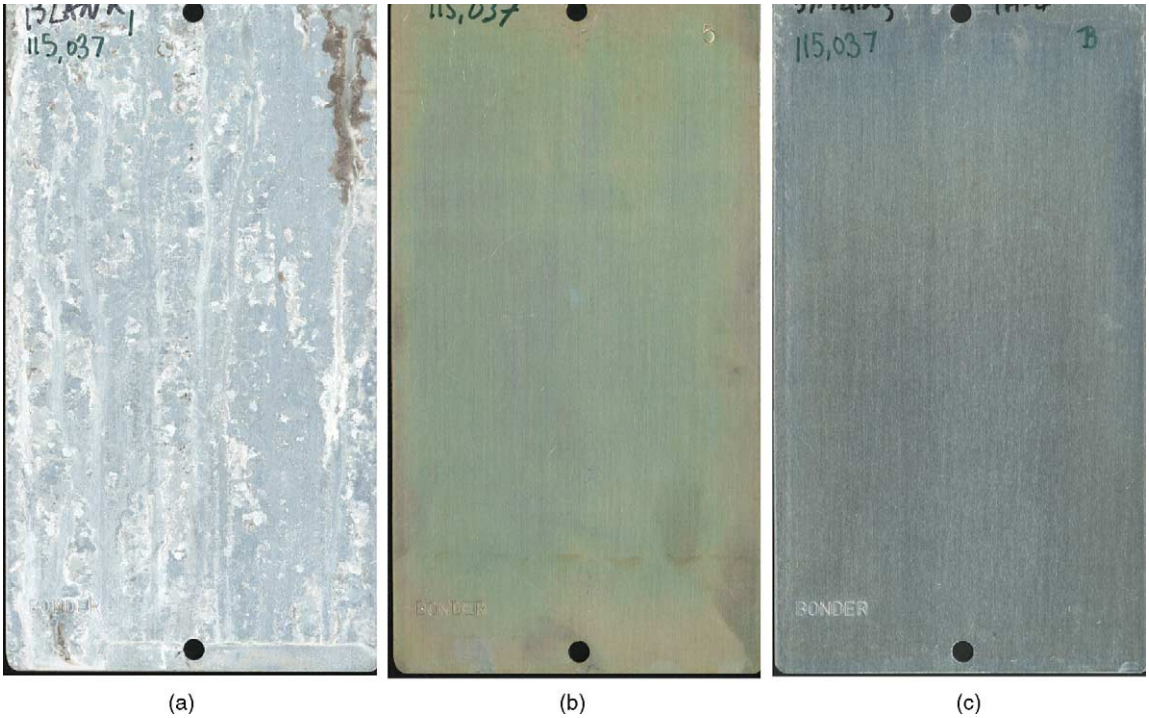

Fig. 4. AA 5005 panels after 336 h of salt spray test: (a) untreated; (b) chromated (Chromicoat 103®); (c) alumina-loaded bis-amino/VTAS silane treated.

metal substrates. The hydrolysis reaction equilibrium in the bis-sulfur silane solution is given by

$$(OR)_3Si(CH_2)_3S_4(CH_2)_3Si(OR)_3 + 6H_2O \Leftrightarrow (OH)_3Si(CH_2)_3S_4(CH_2)_3Si(OH)_3 + 6ROH \quad (3)$$

where S indicates sulfur atom (the subscript 4 is the average number of the S atoms contained in each bis-sulfur silane molecule), OR denotes hydrolyzable alkoxy groups or OC_2H_5 in the case of the bis-sulfur silane, and SiOH indicates silanol. It should be noted that, in reality, this reaction occurs in steps [14], and is not complete when ethanol is used as a solvent for silane solution preparation. The silane film obtained therefore still contains a considerable amount of non-hydrolyzed ester groups [5].

Silica nanoparticles were added into the bis-sulfur silane solution according to the following two-step procedure. First, different amounts of silica (about 1 μm) nanoparticles, i.e. 0.01, 0.03, 0.04 and 0.1 wt.% were mixed with DI water using a high-speed blender until uniform silica colloidal solutions were obtained. The estimated mixing time was around 20 min. Five parts of the silica colloidal solutions were then added into the silane/ethanol mixture at the mixing ratio of 5/90 (v/v). The concentrations of silica nanoparticles in the silane solutions then became 5, 15, 20 and 50 ppm.

Alloy. AA 2024-T3 panels with the dimension of 10 cm × 15 cm × 0.06 cm (width × length × thickness) were purchased from ACT Inc. (Hillsdale, MI).

2.2. Alkaline degreasing and silane surface treatment

The AA 2024-T3 panels were degreased in a diluted alkaline cleaner (AC1055®, provided by Brent America Inc., Lake Bluff, IL) at 65 °C for 3–5 min, rinsed with tap water, and then dried with compressed air. The cleaned panel surfaces were completely "water-break-free" (i.e. thoroughly wettable by water). The cleaned AA 2024-T3 panels were dipped into the hydrolyzed 5% bis-sulfur silane solutions for 30 s, and then cured at 100 °C for 1 h in order to obtain an extensively crosslinked film structure.

2.3. Electrochemical tests

The dc polarization tests were carried out on AA 2024-T3 panels with and without the bis-sulfur silane treatments in an aerated 0.6 M NaCl solution at pH 6.5. The silane-treated panels were pre-immersed in the electrolyte for 24 h before data acquisition, in order to achieve a steady state. The bare AA 2024-T3 panels were tested immediately after exposure to the electrolyte. A commercial saturated calomel electrode (SCE) and a platinum mesh were used as the reference and counter electrodes, respectively. The exposed area was 0.78 cm^2. On the average, three replicate samples were tested for each condition. The data were recorded over the range of $E_{corr} \pm 0.25$ V per SCE (where E_{corr} is the corrosion potential of the tested samples). The scan rate was 1 mV/s.

Electrochemical impedance spectroscopy (EIS) *measurements* were employed to evaluate the corrosion performance of the silane-treated AA 2024-T3 systems in a 0.6 M NaCl solution (pH 6.5). The EIS measurements were carried out using an SR810 frequency response analyzer connected to a Gamry PC-3 potentiostat. The measured frequency range was from 10^{-2} to 10^5 Hz, with an ac excitation amplitude of 10 mV. SCE was used as the reference electrode and coupled with a graphite counter electrode. The surface area exposed to the electrolyte was 5.16 cm^2.

2.4. Mechanical tests

Bis-sulfur silane films with different silica amounts were deposited on mirror-like stainless steel surfaces. Fifteen indentation experiments were performed on the bis-sulfur silane-treated samples using MTS Nanoindenter XP and the patented continuous stiffness measurement (CSM) technique, the details of which are best discussed in [15]. The instrument was enclosed in an environmental chamber located in a lab where the ambient temperature was controlled to within ±1 °C. The samples were placed in the chamber for approximately 12 h prior to testing.

2.5. Ellipsometry thickness measurement

Ellipsometry experiments were performed on mirror-like stainless steel panels deposited with bis-sulfur silane films with different amounts of silica. A wide range of wavelengths of 300–800 nm with angle of incidence at 60, 65, 70, 75°, respectively, were employed. The Psi and the delta values were calculated and a computer was used for data acquisition. Further information about ellipsometry can be referred to [18].

3. Results and discussion

3.1. Electrochemical tests of AA 2024-T3 in a 0.6 M NaCl solution (pH 6.5)

Fig. 5 shows the dc polarization curves of AA 2024-T3 treated with and without bis-sulfur silane. All the silane-treated panels were immersed in the electrolyte for 24 h before testing to reach a steady state, while the untreated panel was tested without delay. Curve 1 represents the untreated AA 2024-T3; while curves 2–4 are for the bis-sulfur silane treated AA 2024-T3 panels but loaded with different amounts of silica nanoparticles in the silane films. It is seen that after being treated with the bis-sulfur silane (curve 2), both anodic and cathodic current densities have been reduced appreciably by at least one decade. The E_{corr} corresponding to the film from 5 ppm silica-containing silane solution

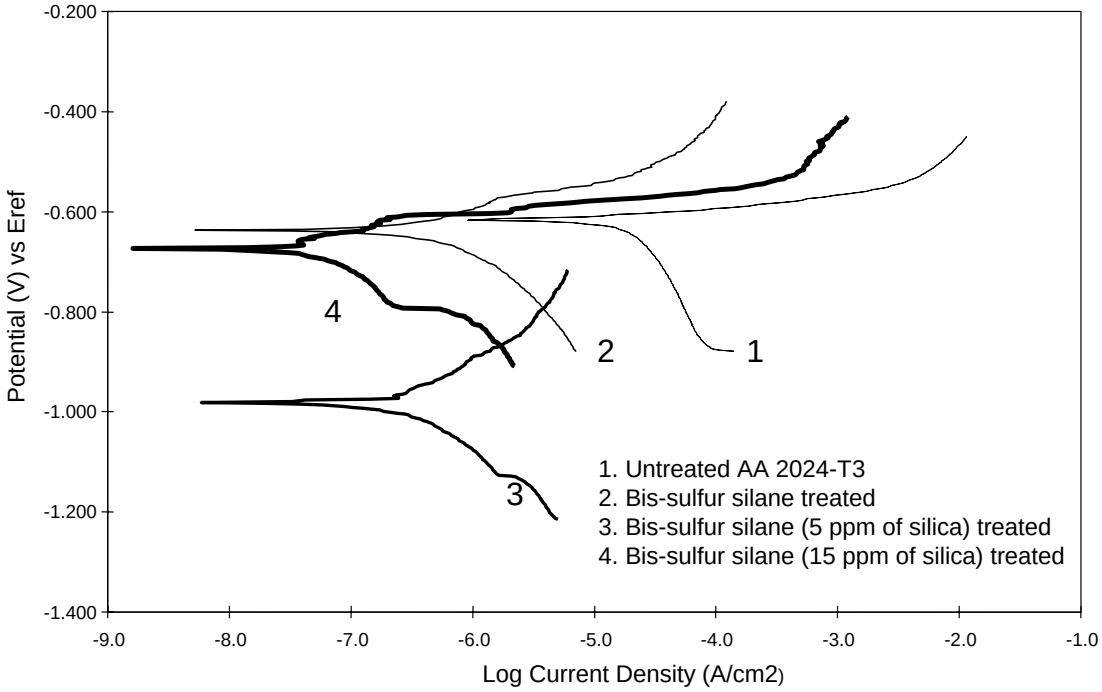

Fig. 5. The dc polarization curves of AA 2024-T3 treated with and without nanoparticle-filled bis-sulfur silane films.

shifts significantly in the cathodic direction, from the original value of −0.6 to −1.0 V per SCE (curve 3). This shift indicates that the incorporation of a small amount of silica particles alters the cathodic kinetics on the alloy surface. When increasing the amount of silica in the silane solution up to 15 ppm, such cathodic shift disappears for the corresponding silane film, with the E_{corr} shifting back to around −0.6 V per SCE (curve 4). Another pronounced feature in Fig. 5 is that two cathodic regions are shown in curves 3 and 4 but not in curves 1 and 2. This further suggests that a small amount of silica particles in the silane film do change the mechanism of cathodic reactions on the alloy surface. Instead of one major cathodic reaction, two cathodic reactions reflected by the two cathodic regions dominate over the applied cathodic voltages. The proposed mechanism is explained later in this paper.

The values of E_{corr} and corrosion rates (I_{corr}) of nano-structured bis-sulfur silane treated AA 2024-T3 systems are plotted as a function of the contents of silica particles in the silane solutions in Fig. 6. A dip in E_{corr} is seen

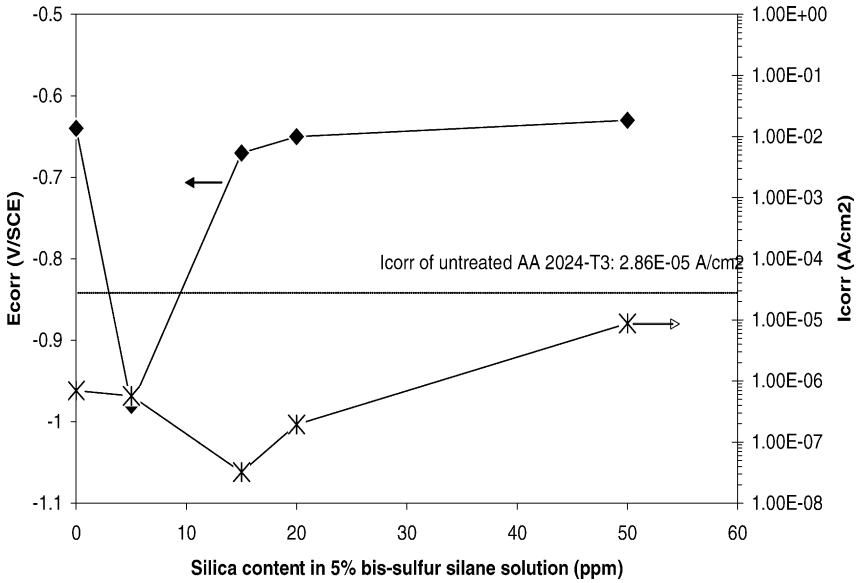

Fig. 6. E_{corr} and I_{corr} of bis-sulfur silane treated AA 2024-T3 systems as a function of silica content in the bis-sulfur silane solution.

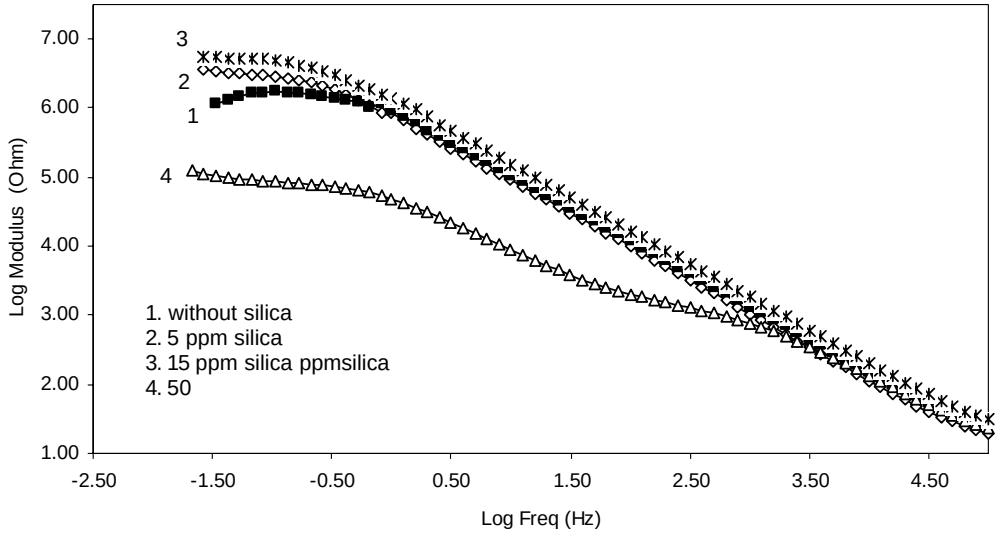

Fig. 7. Impedance plots of bis-sulfur silane treated AA 2024-T3 systems loaded with different amounts of silica nanoparticles.

for the film obtained from the 5 ppm silica-containing silane solution, shifting from −0.63 to −1.0 V per SCE. This indicates that the silane film from the 5 ppm silica-containing silane solution behaves as a cathodic barrier like cerium compounds [16,17]. This nano-structured film surface suppress the cathodic reactions, and therefore inhibits the entire corrosion process in the system. With an increase in silica content up to 15 ppm such cathodic inhibitive behavior disappears, inferring that the bis-sulfur silane film no longer performs as a cathodic inhibitive layer when the silica amount in the film exceeds a certain value.

The trend in the I_{corr} values with increase in silica contents is also shown in Fig. 6. A drop in I_{corr} is observed corresponding to the silica content of 15 ppm in the solution. The I_{corr} values, however, shift back when further increasing the silica content in the solution. At the silica content of 50 ppm, the I_{corr} value for the corresponding silane film exceeds that of the unloaded bis-sulfur silane film and gradually approaches the I_{corr} value for the untreated AA 2024-T3, showing that the corrosion inhibition of the silane film degrades when loaded with too many silica particles.

Fig. 7 compares the EIS behaviors of silica-loaded bis-sulfur silane films deposited on AA 2024-T3. The results were obtained in 0.6 M NaCl solution at pH 6.5. All the panels were immersed in the electrolyte for 24 h before data acquisition. A similar trend is observed here: the low-frequency impedance values (Z_{lf}) of the systems increase with the increase of the silica content until 15 ppm (curves 2 and 3 in Fig. 7) compared with the unloaded panel (curve 1 in Fig. 7). The Z_{lf} value, however, drops sharply for the film obtained from 50 ppm silica-containing silane solution (curve 4 in Fig. 7). This, again, confirms that a large amount of silica particles is not required from the point view of a good corrosion performance of the bis-sulfur silane film. In addition, a two-time-constant behavior is clearly shown in curve 4 corresponding to 50 ppm silica. The time constant at high frequencies is due to the nano-structured silane film, while the one at low frequencies may be attributed to a double layer formed at the silane/metal interface. The formation of the double layer in the 50 ppm silica-loaded silane system indicates that an excess of silica particles in the film has a negative effect on the interfacial adhesion, leading to a premature film delamination from the substrate.

On the basis of the above results, it can be generally concluded that a small amount of silica nanoparticles (e.g. obtained from the silane solution with silica $\leq$15 ppm) does improve the corrosion performance of the bis-sulfur silane film on AA 2024-T3. However, such improvement diminishes when further increasing the silica amount in the film (e.g. silica in the solution >15 ppm). Moreover, an extra large amount of silica particles in the film even degrades the corrosion performance of the silane film (e.g. >50 ppm), as confirmed in both dc and EIS tests. The premature film delamination observed in Fig. 7 is most likely the result of heavy water intrusion due to the increase in the film porosity after loaded with a large amount of silica nanoparticles.

3.2. Thickness dependence of corrosion performance of nanoparticle-filled bis-sulfur silane films on AA 2024-T3

Fig. 8 displays the bis-sulfur silane film thickness and the corresponding I_{corr} values as a function of silica contents in the silane solutions. It is clear in Fig. 8 that the film thickness increases with increasing silica amount in the corresponding silane solutions until 15 ppm, and remains constant afterwards. This indicates that the film is indeed thickened by incorporating silica particles. However, an additional amount of silica cannot thicken the silane film further. It is also noted that a minimum of I_{corr} corresponds to 15 ppm silica where the film thickness achieves its maximum. A further increase in the I_{corr} values seems independent of the film thickness, and a possible explanation was given above.

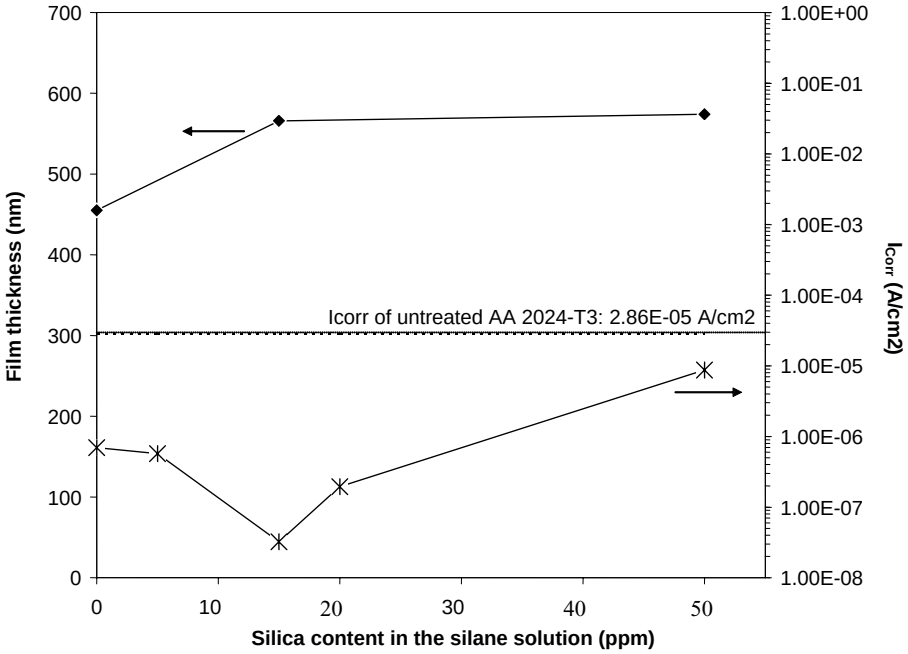

Fig. 8. Film thicknesses and I_{corr} values of the bis-sulfur silane film as a function of silica content in the bis-sulfur silane solution.

3.3. Mechanical properties of nanoparticle-filled bis-sulfur silane films on AA 2024-T3

The values of hardness of the silane films loaded with and without silica nanoparticles are plotted as a function of displacement into the stainless steel substrate surface, as shown in Fig. 9. It is clearly seen that the film hardness increases constantly with the increasing silica amount in the film. Additionally, two distinct regions are also seen in Fig. 9. The region below 200 nm can be considered as the silane surface. The hardness values for all films in this region remain nearly constant. The film corresponding to 50 ppm possesses the highest value, whereas that to 5 ppm does not show any improvement in hardness as compared with the film without silica. When stepping into the second region (i.e. above 200 nm), the hardness values for all silica-containing films increase rapidly with the displacements. According to our previous works [5,12,13], this region is designated as the highly crosslinked interfacial layer comprising covalent bonds of SiOSi and AlOSi. From Fig. 9, it is clearly observed that silica has a significant effect on this region. Even the film obtained from the 5 ppm silica-containing silane

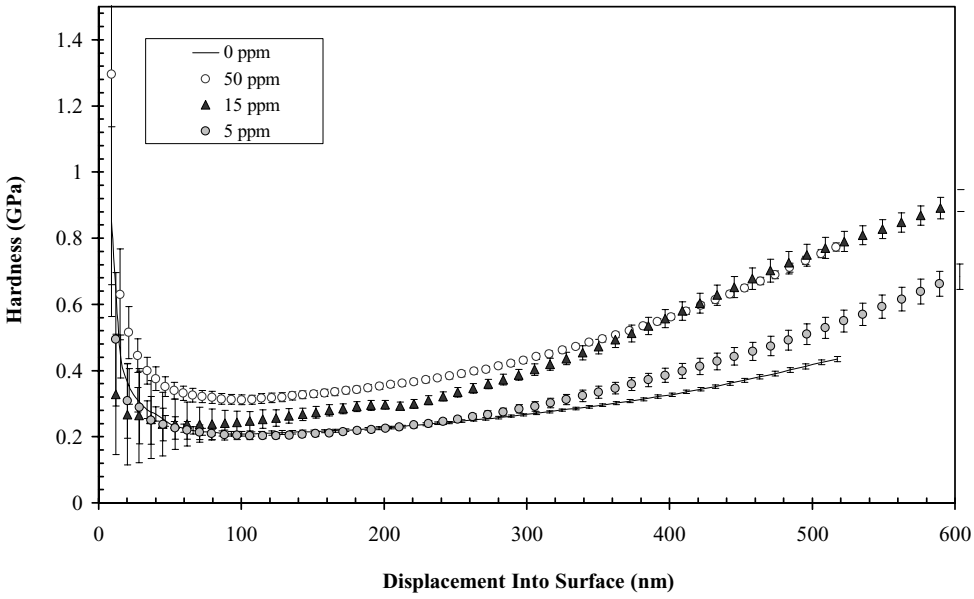

Fig. 9. Hardness of bis-sulfur silane films loaded with and without silica nanoparticles.

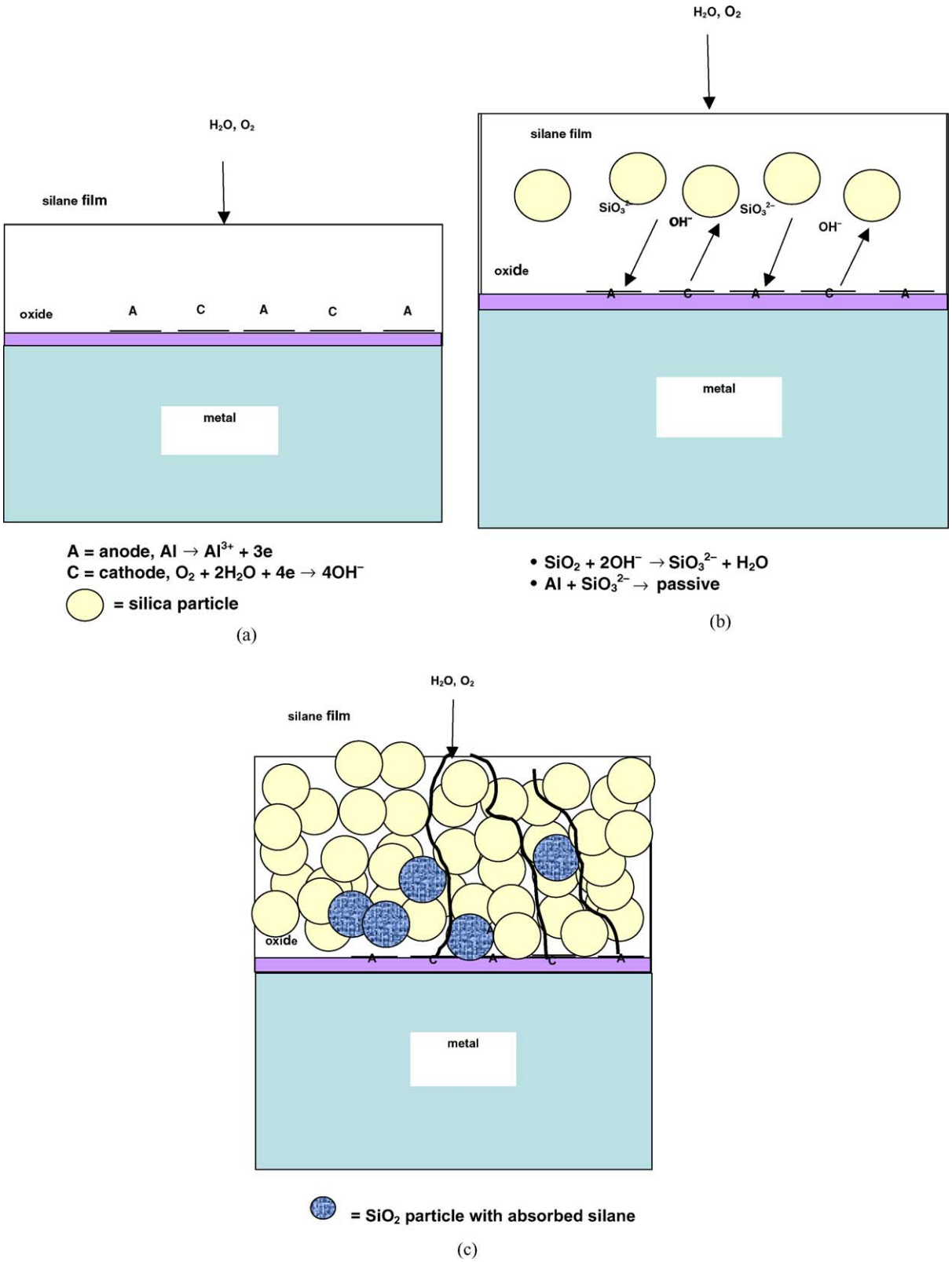

Fig. 10. Model for silica effect on corrosion inhibition: (a) none; (b) low silica; (c) high silica.

solution shows a noticeable improvement in hardness in comparison with the film without silica. The other two films corresponding to 15 and 50 ppm silica exhibit even higher hardness values than that to 5 ppm. It is also noted that the hardness values for the latter two overlap to each other when approaching to the substrate.

Based on the above results, it appears that the interfacial region is preferentially hardened by the incorporation of the silica particles. With a further increase in silica amount (e.g. 15 ppm), not only the interfacial layer but also the silane surface is hardened by showing an improvement in its hardness value. However, an extra amount of silica (e.g. 50 ppm) seems only to strengthen the silane surface but not the interfacial layer, as no further increase is seen for the hardness of the interfacial layer after 15 ppm.

3.4. Proposed inhibition mechanism

In general, the bis-sulfur silane film on loading with silica nanoparticles tends to improve the corrosion and mechanical properties up to a certain extent, beyond which further loading of silica nanoparticles tends to degrade the film. This observed effect is always seen in the paint industry where this critical point is referred to as the critical pigment volume concentration (CPVC), coatings are typically formulated below this critical concentration.

The proposed inhibition mechanism is based on the above principle. Fig. 10 shows the model for the silica effect in the silane film. Fig. 10(a) indicates the silane film with no silica, 'A' refers to anodic sites and 'C' to cathodic sites. When the silane film is loaded with small amounts of silica as shown in Fig. 10(b), the silica suppresses the cathodic reaction (water/oxygen reduction under the experimental conditions in this work) by reacting with the cathodically generated OH^- ions,

$$SiO_2 + 2OH^- \rightarrow {SiO_3}^{2-} + H_2O \quad (4)$$

The as-formed ${SiO_3}^{2-}$ ions react with Al^{3+} ions at the anodes, forming a passive silicate film. Such catholic inhibition is confirmed in the dc polarization test with a shift in E_{corr} to lower values (Fig. 6).

Fig. 10(c) shows the effect of large amounts of silica in the silane film. The silica particles adsorb the silanes and the film becomes more porous. The silica particles start to protrude out of the surface, thus making water penetration easier through the pores in the film. This leads to deterioration of the corrosion properties of the film, an effect similar to the CPVC in the paint industry. Further investigation in the inhibition mechanism is under progress.

4. Conclusions

1. Cathodic reactions can be suppressed by a small amount of silica via reacting with cathodically generated OH^- ions, and later on forming passive Al-silicate compounds. The optimum silica amount in the corresponding silane solutions appears to be between 5 and 15 ppm.
2. Bis-sulfur silane film can be thickened and strengthened by loading silica nanoparticles into the film. The interfacial layer is preferentially hardened by silica. The silane surface is hardened when the silica amount exceeds 15 ppm in the corresponding silane solution. An extra amount of silica further hardens the surface but not the interfacial layer.
3. Although the incorporation of an extra amount of silica nanoparticles into the bis-sulfur silane film further improves the film hardness, it seemed to degrade the corrosion performance of the film. The EIS results indicated that the bis-sulfur silane film heavily loaded with silica nanoparticles tends to form a porous film, which promotes electrolyte intrusion into the system, causing a premature film delamination.

Acknowledgements

The authors are grateful for the financial support from Chemat Inc., for the assistance of Matt Stacy at the University of Cincinnati for film thickness measurement and Dan Plazk at MTS for mechanical testing. The authors would also like to acknowledge the financial support for this work by the Air Force Office of Scientific Research under contract F49620-01-1-0352.

References

[1] W.J. Van Ooij, T.F. Child, Chemtech 28 (1998) 26.
[2] V. Subramanian, Ph.D. Dissertation, Department of Materials Science and Engineering, University of Cincinnati, 1999.
[3] G.P. Sundararajan, M.S. Thesis, Department of Materials Science and Engineering, University of Cincinnati, 2000.
[4] W.J. Van Ooij, D. Zhu, G.P. Sundararajan, S.K. Jayaseelan, Y. Fu, N. Teredesai, Surf. Eng. 16 (2000) 386.
[5] W.J. Van Ooij, D. Zhu, Corrosion 157 (2001) 413.
[6] M.A. Petrunin, A.P. Nazarov, Yu.N. Mikhailovski, J. Electrochem. Soc. 143 (1999) 251.
[7] A.M. Beccaria, L. Chiaruttini, Corros. Sci. 41 (1999) 885.
[8] P.R. Underhill, D.L. Duquesnay, K.L. Mittal (Eds.), Silanes and Other Coupling Agents, vol. 2, VSP, Utrecht, 2000, p. 149.
[9] E.P. Plueddemann, Silane Coupling Agents, 2nd ed., Plenum Press, New York, 1991.
[10] K.L. Mittal (Ed.), Silanes and Other Coupling Agents, VSP, Utrecht, 1992.
[11] K.L. Mittal (Ed.), Silanes and Other Coupling Agents, vol. 2, VSP, Utrecht, 2000.
[12] D. Zhu, W.J. Van Ooij, Corros. Sci. (2003) 2177.
[13] D. Zhu, W.J. Van Ooij, J. Adhes. Sci. Technol. 16 (2002) 1235.
[14] F.D. Osterholtz, E.R. Pohl, J. Adhes. Sci. Technol. 6 (1992) 127.
[15] W.C. Oliver, G.M. Pharr, J. Mater. Res. 7 (1992) 1564.
[16] R.L. Parkhill, E.T. Knobbe, M.S. Donley, Prog. Org. Coat. 41 (2001) 261.
[17] E. Morris, J.O. Stoffer, T.J. O'Keefe, P. Yu, X. Lin, Polym. Mater. Sci. Eng. 81 (1999) 167.
[18] R.M.A. Azzam, N.M. Bashara, Ellipsometry and Polarized Light, North-Holland, Amsterdam, 1977.